Overexpression screens identify conserved dosage chromosome instability genes in yeast and human cancer

Supipi Duffy[a], Hok Khim Fam[b,c], Yi Kan Wang[d], Erin B. Styles[e,f], Jung-Hyun Kim[g], J. Sidney Ang[a], Tejomayee Singh[a], Vladimir Larionov[g], Sohrab P. Shah[d], Brenda Andrews[e,f], Cornelius F. Boerkoel[b,c], and Philip Hieter[a,c,1]

[a]Michael Smith Laboratories, University of British Columbia, Vancouver, BC, Canada V6T 1Z4; [b]Child and Family Research Institute, University of British Columbia, Vancouver, BC, Canada V5Z 4H4; [c]Department of Medical Genetics, University of British Columbia, Vancouver, BC, Canada V6T 1Z3; [d]BC Cancer Agency, Vancouver, BC, Canada V5Z 4E6; [e]Department of Molecular Genetics, University of Toronto, Toronto, ON, Canada M5S 1A8; [f]The Donnelly Centre for Cellular and Biomolecular Research, University of Toronto, Toronto, ON, Canada M5S 3E1; and [g]Center for Cancer Research, National Cancer Institute, Bethesda, MD 20892

This contribution is part of the special series of Inaugural Articles by members of the National Academy of Sciences elected in 2016.

Contributed by Philip Hieter, July 25, 2016 (sent for review May 26, 2016; reviewed by Thomas D. Petes and Jasper Rine)

Somatic copy number amplification and gene overexpression are common features of many cancers. To determine the role of gene overexpression on chromosome instability (CIN), we performed genome-wide screens in the budding yeast for yeast genes that cause CIN when overexpressed, a phenotype we refer to as dosage CIN (dCIN), and identified 245 dCIN genes. This catalog of genes reveals human orthologs known to be recurrently overexpressed and/or amplified in tumors. We show that two genes, *TDP1*, a tyrosyl-DNA-phosphdiesterase, and *TAF12*, an RNA polymerase II TATA-box binding factor, cause CIN when overexpressed in human cells. Rhabdomyosarcoma lines with elevated human Tdp1 levels also exhibit CIN that can be partially rescued by siRNA-mediated knockdown of *TDP1*. Overexpression of dCIN genes represents a genetic vulnerability that could be leveraged for selective killing of cancer cells through targeting of an unlinked synthetic dosage lethal (SDL) partner. Using SDL screens in yeast, we identified a set of genes that when deleted specifically kill cells with high levels of Tdp1. One gene was the histone deacetylase *RPD3*, for which there are known inhibitors. Both HT1080 cells overexpressing h*TDP1* and rhabdomyosarcoma cells with elevated levels of hTdp1 were more sensitive to histone deacetylase inhibitors valproic acid (VPA) and trichostatin A (TSA), recapitulating the SDL interaction in human cells and suggesting VPA and TSA as potential therapeutic agents for tumors with elevated levels of hTdp1. The catalog of dCIN genes presented here provides a candidate list to identify genes that cause CIN when overexpressed in cancer, which can then be leveraged through SDL to selectively target tumors.

dosage chromosome instability | overexpression | synthetic dosage lethality | TDP1 | rhabdomyosarcoma

Chromosome instability (CIN) is an inherent enabling characteristic of cancer important for tumor initiation and progression and is observed in a majority of tumors (1–3). It has been proposed that alterations resulting in genome instability happen early during tumor formation, allowing the accumulation of errors during DNA replication, repair, and chromosome segregation, thereby increasing the likelihood that a cell will acquire multiple genetic changes necessary for tumor progression (4). CIN is possibly the major contributor to intratumoral heterogeneity—that is, the presence of genetically distinct populations of cells within a single tumor that impacts treatment strategy, drug resistance, and tumor evolution (5–8). For these reasons, defining genes and pathways that drive CIN and understanding the mechanisms that underlie genome stability will contribute not only to an understanding of tumor etiology and progression but will also be relevant for guiding therapeutic strategies. The budding yeast *Saccharomyces cerevisiae* has served as an excellent model system for studying highly conserved biological pathways and has been instrumental in delineating pathways involved in genome instability (9). Although the complete spectrum of genes that are mutable to a CIN phenotype [loss-of-function (LOF) and reduction-of-function (ROF) alleles] have been determined in yeast (10, 11), the spectrum of genes that when amplified or overexpressed cause CIN are less well-defined (12, 13).

Somatic copy number amplifications (SCNAs) are one of the most prevalent genetic alterations in cancer genomes (14). The high frequency of recurring SCNAs suggests that some SCNAs may be cancer drivers and emphasizes the need to uncover driver genes within these regions (15). However, as amplified regions often encompass multiple genes, defining potential driver genes on SCNAs and distinguishing driver SCNA events are major challenges (16, 17). Consequently, oncogenes and tumor suppressor genes have only been defined within few (<30%) recurrently altered regions in tumor genomes (17), leaving a significant opportunity to identify novel genes in these regions that can promote tumor biology and progression.

Genetic alterations that cause CIN not only drive tumorigenesis but also present vulnerabilities that can be leveraged to selectively kill tumor cells. One approach involves exploiting synthetic lethal interactions with CIN gene alterations. The concept of synthetic

Significance

Chromosome instability (CIN) is well established as an enabling characteristic of cancer that contributes to cancer initiation and progression. Here, we identify 245 genes whose individual overexpression causes CIN in yeast, and we show that the overexpression of several of these dosage CIN (dCIN) genes also causes CIN in human cells. We demonstrate that genetic screens in yeast can be used to determine candidate target genes for specific killing of cancer cells overexpressing dCIN genes. Rhabdomyosarcoma cells with elevated levels of Tdp1 are one example where the histone deacetylase inhibitors valproic acid and trichostatin A can be used to specifically kill these cells. We have generated a list of dCIN candidate genes that can facilitate selective targeting of tumor cells.

Author contributions: S.D. and P.H. designed research; S.D., H.K.F., E.B.S., J.S.A., and T.S. performed research; S.D., H.K.F., Y.K.W., E.B.S., J.-H.K., V.L., B.A., and C.F.B. contributed new reagents/analytic tools; S.D., H.K.F., Y.K.W., and S.P.S. analyzed data; and S.D. and P.H. wrote the paper.

Reviewers: T.D.P., Duke University Medical Center; and J.R., University of California, Berkeley.

The authors declare no conflict of interest.

Freely available online through the PNAS open access option.

[1]To whom correspondence should be addressed. Email: hieter@msl.ubc.ca.

This article contains supporting information online at www.pnas.org/lookup/suppl/doi:10.1073/pnas.1611839113/-/DCSupplemental.

lethality (SL), where combining the mutations of two genes results in significantly lower fitness compared with mutating each gene individually, has been explored previously as a therapeutic approach for the selective targeting of tumors with gene mutations that cause CIN (18–23). The SL interaction between mutations in the genome stability genes *BRCA1* and *BRCA2* and inhibitors of *PARP* is one such example (24, 25). Most SL approaches focus on exploiting specific somatic mutations or deletions in cancer driver genes; however, there are just as many amplified regions as deleted regions in cancer genomes (17). Thus, we propose using synthetic dosage lethality (SDL), which is SL with an amplified and/or overexpressed gene, as an approach to selectively target tumors that overexpress dCIN genes (26, 27). SDL occurs when the overexpression of a gene is not lethal in a wild-type background but in conjunction with a second site nonlethal mutation causes lethality (28–30). Given that both amplifications and deletions are equally important determinants that drive tumor progression (31), targeting dCIN genes can greatly expand the number of tumors that can be treated with an SL-based approach.

Here we describe genome-wide screens in yeast identifying 245 dCIN genes, 237 of which are previously unidentified. To demonstrate the utility of this resource, we searched for candidate human orthologs of yeast dCIN genes that are recurrently amplified and/or overexpressed in tumors and found four genes that recapitulated a dCIN phenotype. The expression of one such conserved human dCIN gene, *TDP1*, is elevated in rhabdomyosarcoma (RMS) cells that exhibit CIN, and the CIN phenotype is partially rescued by siRNA-mediated knockdown of Tdp1. Tdp1 is a tyrosyl-DNA-phosphodiesterase (32) responsible for hydrolyzing Topoisomerase 1 (Top1)–DNA adducts that occur when Top1 becomes covalently trapped on the DNA, which often happens when cells are treated with the Top1 poison camptothecin (CPT) (33–36). We then screened *TDP1* overexpression in yeast for SDL partner genes and found several interactions, which identify potential therapeutic targets for tumors overexpressing hTdp1. The histone deacetylase (HDAC) *RPD3* was one candidate gene, and we show that both HT1080 cells overexpressing hTdp1 and RMS cells with elevated levels of hTdp1 are more sensitive to the HDAC inhibitors valproic acid (VPA) and trichostatin A (TSA). Our study expands the view of gene overexpression causing CIN and provides a valuable resource for identifying candidate dCIN genes in humans. In addition, we demonstrate that dCIN genes represent genetic vulnerabilities that could be exploited by SDL to selectively kill cancer cells.

Results

Systematic Gene Overexpression in Yeast Identifies 245 Dosage CIN Genes. To discover genes that when overexpressed result in CIN, we screened an arrayed collection of 5,100 yeast strains, each conditionally overexpressing a unique gene under the control of a galactose-inducible promoter (37), using two different assays: Chromosome Transmission Fidelity (CTF), which monitors the inheritance of an artificial chromosome fragment (CF) (11, 38), and A-Like Faker (ALF), which measures the loss of the *MATα* locus, thereby allowing haploid cells to mate with a tester strain of the same mating type (11, 39) (Fig. S1). These screens identified 245 genes that when overexpressed increased CIN in at least one of the assays. Of the 245 dosage CIN (dCIN) genes, 108 dCIN genes (44%) were identified in both the ALF and CTF screens, and 44 dCIN genes (18%) and 93 dCIN genes (38%) were specific to either the CTF or the ALF screens, respectively. These differences likely reflect the different types of CIN detected by the two assays, as CTF predominantly measures whole chromosome loss whereas ALF detects chromosome loss, chromosome rearrangement, and gene conversion events (10, 11).

The list of dCIN genes presented in Fig. 1*A* and Table S1 were analyzed for general characteristics (see *Materials and Methods* for details on validation). dCIN genes were enriched for diverse processes including cell division, chromosome segregation, transcription, and response to DNA damage (Fig. 1*B*). When grouped by biological function based on *Saccharomyces* Genome Database (SGD) and Gene Ontology (GO), a high proportion of dCIN genes encode proteins that associate with nuclear processes and localize to the nucleus (Fig. 1*C*). Approximately 30% of the dCIN genes belong to biological pathways not typically associated with CIN, similar to as observed for CIN genes (10, 11); thus, the mechanisms of dCIN will require further experiments.

Our screens have extended the list of 55 previously known dCIN genes by more than fourfold for a total of 290 genes that cause CIN when overexpressed (12, 13, 40, 41).

Analysis of the dCIN Gene Catalog Uncovers Multiple Mechanisms Behind dCIN. Although it is clear how loss or reduction of a cellular component leads to a phenotype like CIN, there are fewer examples of how overexpression might affect the chromosomal equilibrium. As our catalog of dCIN genes represents a resource on the effect of overexpression on chromosome stability, we were interested in exploring the underlying characteristics of the phenotype. First, we compared our list of 245 dCIN genes to 692 CIN genes whose loss of function (LOF) or reduction of function (ROF) has previously been identified as increasing genome instability (10, 11). Sixty-seven genes were common to both the CIN and dCIN gene datasets (Fig. 2*A* and Table S2), suggesting that the overexpression of the dCIN gene may phenocopy LOF. To test whether this concordance between overexpression and LOF or ROF mutations is limited to CIN or holds true for other phenotypes, we tested whether genes that were both CIN and dCIN share negative genetic interactions. Negative genetic interactions such as synthetic slow growth (SS) or SL occur when the observed fitness defects of a double mutant is less than expected based on the fitness of the two single mutants (Fig. 2*B*) (42). Each of the 67 CIN/dCIN genes was tested for SL/SS interactions with two synthetic lethal partners that were identified in the SGD or the Data Repository of Yeast Genetic Interactions (DRYGIN) database (43) to determine whether the synthetic lethal effect was recapitulated upon overexpression of the dCIN gene. Deletion mutant strains of the SL partners were transformed with plasmids that overexpressed dCIN genes and assayed for fitness using serial spot dilutions (Fig. 2*C*). Overexpression of 32 of the 67 CIN/dCIN genes recapitulated a negative genetic interaction, suggesting that in these cases overexpression may phenocopy LOF (Table S2).

To further assess concurrence between overexpression and LOF or ROF, we chose to examine the sensitivity of strains overexpressing dCIN genes to DNA-damaging agents (DDAs), as many of the CIN gene LOF and ROF mutations cause sensitivity to DDAs. When tested for sensitivity to four genotoxic agents—hydroxyurea (HU), methyl methanesulfonate (MMS), bleomycin, and benomyl—20 of the dCIN/CIN genes caused hypersensitivity to at least one genotoxic agent, but the sensitivity profiles were not identical to LOF/ROF mutations (Table S3). For example, LOF mutants of *RAD27* are sensitive to both HU and MMS, whereas the *RAD27* overexpression allele caused sensitivity to HU, MMS, and also bleomycin. Forty-nine additional dCIN genes caused sensitivity to at least one DDA. In total, overexpression of 69 dCIN genes limits the cell's ability to respond to DDAs and/or may increase cellular DNA damage.

Finally, we assayed the dCIN genes for the presence of increased DNA damage using Rad52 as a marker for DNA double-stranded breaks (DSBs), as DNA damage and defective DNA repair are well-established mechanisms that lead to CIN (44). Previous screens have looked at the effects of LOF (45) and ROF alleles (46) on Rad52-foci formation; however, our study looks at effects of gene overexpression on Rad52-foci formation.

Using synthetic genetic array (SGA) technology (47), we introduced the 245 dCIN overexpression plasmids individually into a reporter strain containing GFP-tagged Rad52 that marked DNA damage sites and mCherry-tagged histone H2A that marked the nuclei (Fig. 2*D*). Spontaneous Rad52 foci were quantified using automated image analysis (see *Materials and Methods*). dCIN genes that exhibited foci in more than 10% of the cells (Table S3), a twofold elevation above the vector-alone controls, were retested as follows: Plasmids were introduced into the Rad52 reporter

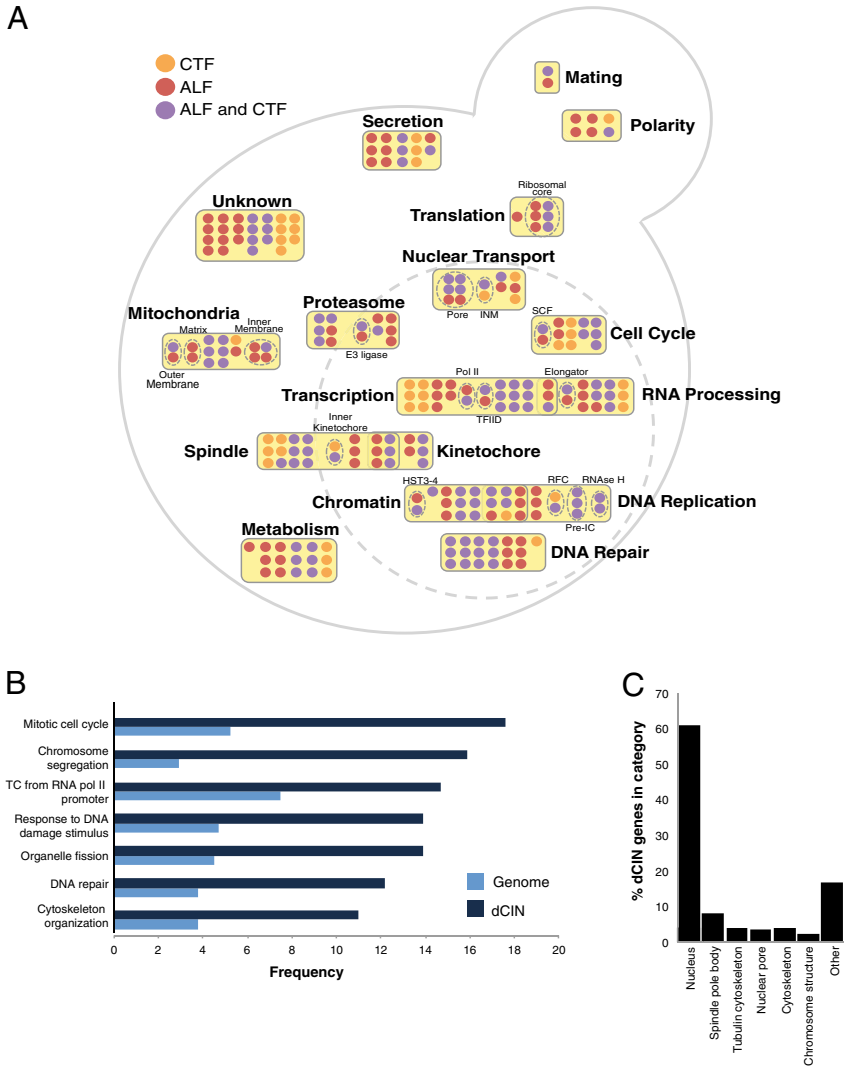

Fig. 1. dCIN genes in yeast. (*A*) A schematic of the 245 dCIN genes arranged according to function (Table S1). Colors of the circles indicate the screens in which genes were identified: ALF (red), CTF (yellow), and both (purple). The large dotted circle denotes the nucleus. Bold labels and yellow boxes represent groups, and the dotted circles indicate protein complexes. Subgroup abbreviations: INM, inner nuclear membrane; Pol II, RNA polymerase II; Pre-IC, preinitiation complex; RFC, Replication Factor C; SCF, Skp, Cullin, F-box containing complex; TFIID, Transcription factor II D. (*B*) Bar graph showing enrichment of the dCIN genes for biological process as defined by GO annotations (dark blue bars) relative to the genome (light blue bars). All associated *P* values are <0.001. (*C*) Cellular localizations of the 245 dCIN genes as determined using SGD.

strain using direct transformations, and foci were imaged using fluorescence microscopy and counted manually. After scoring images from three independent transformants for each dCIN gene, we identified 20 genes whose overexpression increased Rad52 foci (Fig. 2 *E* and *F* and Table S3). Nine of these genes were represented in the 67 CIN/dCIN overlap gene set. A majority of the 20 genes with increased Rad52 foci belong to biological pathways previously linked to DNA metabolism (45). We also identified several genes with no previous links to DNA damage, such as *PAM1*, *SHE9*, *PUS1*, and *KIP3*, implying that a genome-wide overexpression screen for Rad52 foci may identify additional genes involved in DNA metabolism. The increased Rad52 foci in some dCIN strains suggest a requirement for Rad52 for viability. To test if Rad52 function was required, we introduced the 20 dCIN genes that exhibited increased Rad52 foci using direct transformations into a *RAD52* deletion strain and assayed for SDL using serial spot dilutions. Four genes (*CDC6*, *SLK19*, *PSO2*, *RRM3*) when overexpressed in the *rad52*Δ resulted in SDL, suggesting that strains overexpressing these genes require homologous recombination for viability (Fig. 2*G*).

Our analysis of the 67 genes common to both the CIN and the dCIN datasets shows that for a subset of 23 genes, the phenotypic concurrence was limited to the CIN phenotype. Overexpressing 32 of the 67 CIN/dCIN genes recapitulated a negative genetic interaction, 20 were hypersensitive to at least one genotoxic agent, and nine increased Rad52 foci (Tables S2 and S3). For this set of 44 genes that showed concurrence when tested for multiple phenotypes, gene overexpression may result in LOF or ROF.

Testing Candidate dCIN Genes Amplified and/or Overexpressed in Cancer Identifies *TDP1* and *TAF12* as dCIN Genes in Human Cells. Similar to previous candidate-based studies that identified CIN genes in human cells based on phenotypic data from yeast (10, 48), we hypothesized that the dCIN gene list could be used to direct the search for dCIN-associated amplifications in tumors. We generated a list of 292 candidate human dCIN genes using sequence homology to yeast dCIN genes (49, 50) (Table S4). Only two of the 292 genes, *CCNE1* and *CCND1*, have been previously directly linked to dCIN in human cells (51, 52). Based on this list

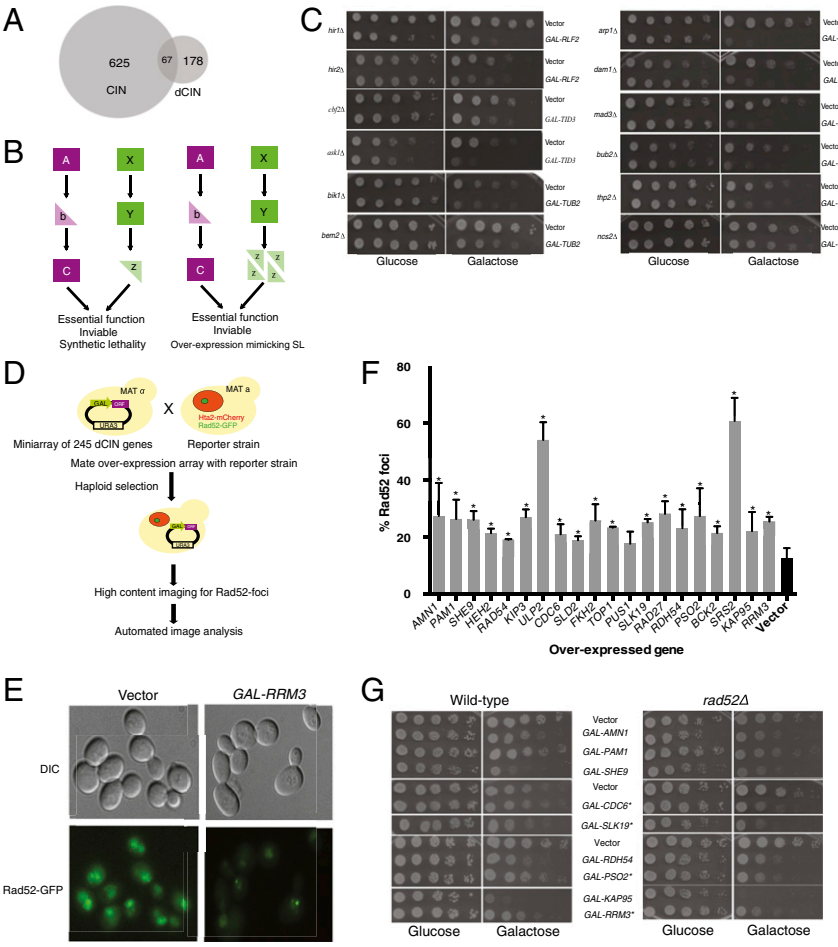

Fig. 2. Comparing dCIN genes to CIN genes. (*A*) Overlap between the dCIN and the CIN gene datasets. (*B*) Negative genetic interactions or SL (*Left*) can occur between parallel nonessential pathways when they converge on a common essential biological process. When overexpression results in LOF of a protein (*Right*), disruption of a parallel pathway similarly will lead to SDL, recapitulating a negative genetic interaction. (*C*) Sample serial spot dilutions of deletion strains transformed with overexpression plasmids and a vector control on glucose and galactose containing media. (*D*) A schematic of the Rad52-foci screen. A mini array containing the 245 dCIN genes were mated to a reporter strain with Rad52-GFP to identify DNA damage foci and Hta2-mcherry, which marks the nucleus. Following the generation of a haploid output array, where every overexpression plasmid contained the two reporter genes, cells were inoculated to liquid media in 96-well plates. Before imaging, overexpression was induced by growing cells in 2% galactose for 6 h. A high-content imaging platform and automated image analysis were used to identify initial hits. (*E*) Sample images from the Rad52-foci confirmations. The reporter strain was transformed with vector-alone control or a plasmid overexpressing *RRM3* grown in galactose for 16 h. Rad52-foci were detected using fluorescence microscopy. (*F*) dCIN genes that show increased Rad52 foci upon overexpression. Each plasmid was directly transformed into a reporter strain with Rad52-GFP and Hta2-mcherry following image acquisition. Data from three independent experiments, each counting >100 cells, are shown (*$P < 0.05$). (*G*) Genetic interactions between the dCIN genes that induce Rad52 foci and cells lacking *RAD52*. Plasmids were directly transformed into either a wild-type strain or a *rad52*Δ and tested using serial spot dilutions. Genes that showed an SDL interaction are marked with an asterisk (*).

of dCIN genes, we then chose 20 candidate genes for functional testing in human cells (Table S4).

The dCIN phenotype in human cells was examined using a quantitative assay based on a nonessential human artificial chromosome (HAC) (53) (Fig. 3*A*). The HAC, which contains *EGFP* (enhanced green fluorescence protein), is maintained as a nonessential chromosome in HT1080 cells due to the presence of a functional kinetochore. Cells that inherit the HAC fluoresce green, whereas HAC loss leads to a loss of fluorescence that can be detected using flow cytometry. HT1080 HAC-GFP lines overexpressing candidate genes were constructed using a lentiviral expression vector (54), and expression of the dCIN candidates was confirmed by Western blots (Fig. S2*A*).

The HAC-based assay can detect CIN induced by chemical agents that destabilize chromosomes (53) but had yet to be tested with genetic perturbations. As a proof-of-principle experiment, we overexpressed *CCNE2* and *CCND1*, two known human dCIN genes, in HAC-GFP–containing cells. Samples were analyzed using flow cytometry every 7 d for a total of 28 d to determine the proportion of nonfluorescent cells. Overexpression of both Cyclin E2 and Cyclin D1 induced HAC loss compared with a vector-only control (Fig. 3*B*). The difference between the control and cyclin overexpression was clearly distinguishable after 14 d and was even more evident after 28 d (Fig. S2*B*). The fraction of cells without the HAC-GFP in the control line agreed well with previous studies (53). We further confirmed that loss of fluorescence detected by flow cytometry corresponds with HAC loss events using fluorescent in situ hybridization (Fig. S2*C*).

Next we tested 18 high-priority candidate genes using the HAC-GFP assay (Fig. S2*D* and *Materials and Methods*). Overexpression of human *TAF12* and *TDP1* increased the loss of the HAC-GFP compared with the vector-alone control (Fig. 3*B*). Human Taf12 (hTaf12) is an RNA polymerase II TATA box-binding factor involved in transcription and was recently identified as an oncogene in brain tumors (55). Elevated hTdp1 levels are seen in certain rhabdomyosarcomas (RMSs) (56), Dukes C colorectal cancer (57), and nonsmall cell lung cancer (58). Neither of these genes has been previously linked to CIN in human cells.

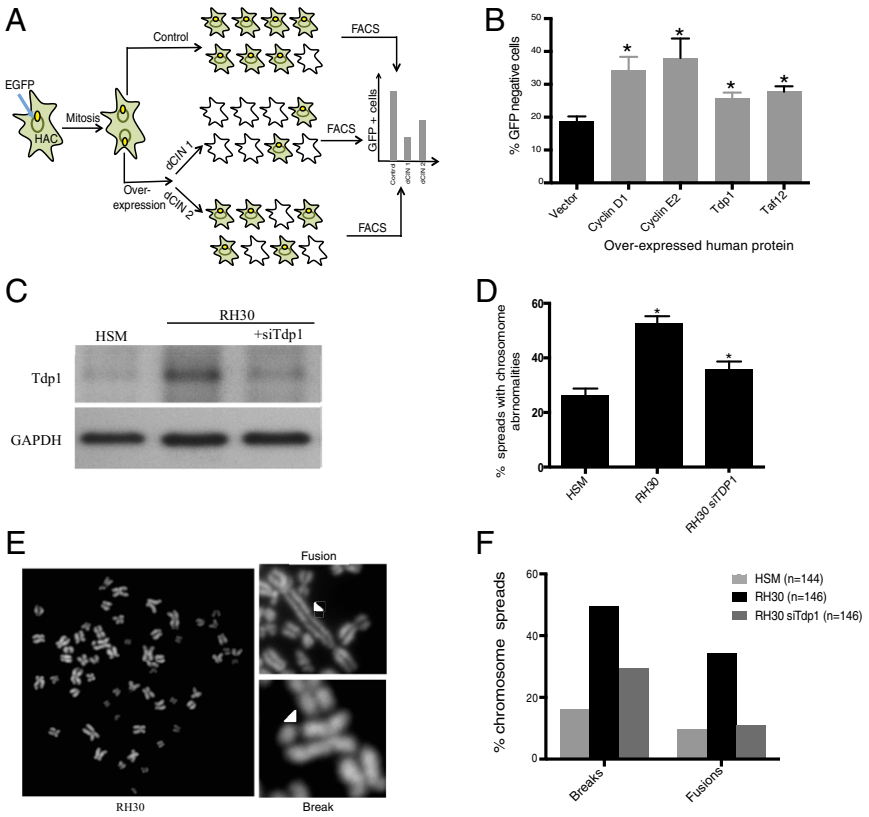

Fig. 3. Recapitulating dCIN in human cells. (*A*) A schematic outlining the HAC-based CIN assay in human cells. Candidate human dCIN genes were overexpressed in HT1080 containing the HAC-GFP, and loss of the HAC, which results in the loss of GFP signal, was quantified using flow cytometry. (*B*) Overexpressing Cyclin D1, Cyclin E2, Tdp1, and Taf12 (light gray bars) compared with HAC-GFP cells overexpressing a vector-only (black) control. Data from three independent experiments are shown in the figure (*P values < 0.05). (*C*) Tdp1 expression levels in RMS (RH30) cells with or without *TDP1* knockdown relative to control cells (HSM). (*D*) CIN observed by metaphase chromosome spreads in RH30 cells and RH30 cells with knockdown of *TDP1* relative to a control. Average values from three replicate experiments are shown (*P < 0.05). (*E*) Representative chromosome spreads and sample images indicating the types of chromosome abnormalities assessed. (*F*) Types of CIN detected in RMS cells with high Tdp1 levels.

RMS Lines Expressing Higher Levels of Tdp1 Show CIN. To further explore the link between increased hTdp1 expression and CIN, we focused on RMS, one of the most common soft tissue sarcomas in children (59). Some RMS tumors have elevated hTdp1 at both the mRNA and protein levels (56). Using metaphase spreads, we examined whether elevated hTdp1 levels caused CIN in RMS cells by comparing chromosomal abnormalities in RH30 cells, which have high levels of Tdp1 relative to control human skeletal muscle (HSM) cells (56). As shown in Fig. 3*D*, in RH30 cells we detected double the percentage of cells with at least one chromosomal abnormality compared with HSM control cells. Chromosome defects observed included chromosome fusions and breaks predominantly, both of which were significantly increased in RH30 cells (Fig. 3 *E* and *F*). Consistent with Tdp1 levels being responsible for the CIN phenotype, the increase in CIN can be reduced by the knockdown of *TDP1* by siRNA (Fig. 3 *C* and *D*).

A SDL Screen for *TDP1* in Yeast to Identify Candidate Targets for Inhibiting Growth of Cancer Cells with Elevated Tdp1 Levels. Given the conservation of the Tdp1 dCIN phenotype in yeast and human tumors, we were interested in understanding Tdp1-induced dCIN and its potential as a target for therapeutics.

In yeast, loss of Tdp1 has no effect on viability, sensitivity to CPT, or CIN (11, 60–63). Deletion of *TDP1* was reported to cause sensitivity to CPT in one high-throughput study (64), however direct tests in several laboratories show that *tdp1*Δ mutants are not sensitive to CPT (61, 65). In contrast, we found that overexpression of yeast Tdp1 causes CIN and sensitivity to the DDAs HU and MMS, suggesting that the overexpression phenotype is distinct from the LOF phenotype (Fig. 4*A*). We also overexpressed a point mutant $Tdp1^{H432R}$ in yeast, which corresponds to the missense mutation in human *TDP1* that causes the neurodegenerative disorder spinocerebellar ataxia with axonal neuropathy (SCAN1) (66, 67). This mutation (H493R) in humans reduces enzyme activity

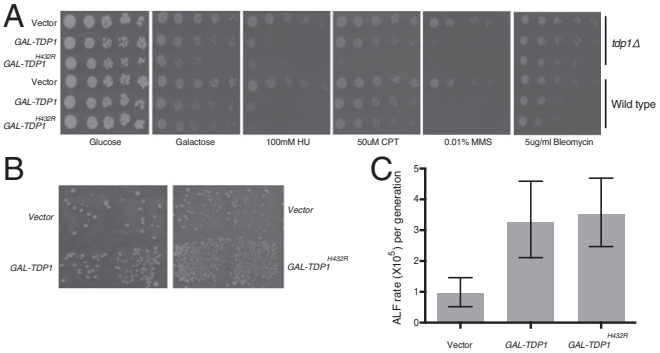

Fig. 4. Tdp1 overexpresssion is distinct from *tdp1*Δ. (*A*) Serial spot dilutions for yeast overexpressing *TDP1* and $TDP1^{H432R}$ in either a wild-type or a strain deleted for *TDP1* in dimethyl sulfoxide (DMSO) control or DDAs MMS (0.001% MMS), HU (100 mM HU), and camptotecin (50 μM CPT) compared with a vector alone. (*B*) The ALF phenotype of Tdp1 and the $Tdp1^{H432R}$ mutant. (*C*) Quantitative ALF assay to assess dCIN after overexpression of *TDP1* and $TDP1^{H432R}$ mutants. Error bars represent 95% confidence intervals.

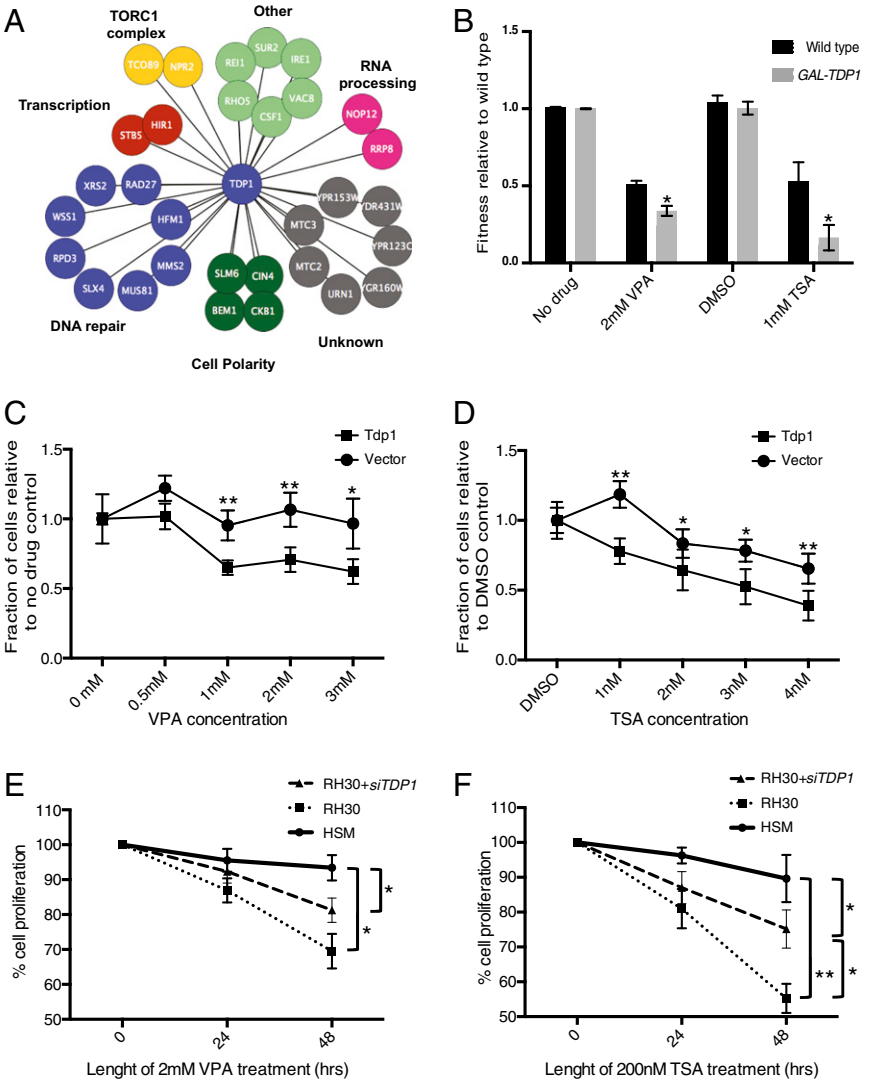

Fig. 5. A SDL screen for Tdp1. (*A*) Validated SDL interactions for yeast Tdp1. Genes are grouped according to biological processes as annotated by Costanzo et al. (43). A complete list of SDL interactions is provided in Table S5. (*B*) Liquid growth curve data for yeast cells carrying a vector-alone control or overexpressing *TDP1* were grown in media containing two HDACIs, 2 mM VPA and 1 mM TSA, along with the corresponding no-drug controls (H_2O for VPA and DMSO for TSA). *$P <$ 0.05. (*C*) HT1080-HAC cells carrying a vector-alone control or overexpressing *TDP1* were exposed to several concentrations of VPA. Fractions of cells relative to the no-drug control are shown at the various concentrations. *$P < 0.05$, **$P < 0.005$. (*D*) HT1080-HAC cells carrying a vector-alone control or overexpressing *TDP1* were exposed to several concentrations of TSA. Fractions of cells relative to the DMSO control are shown at the various concentrations. *$P < 0.05$, **$P < 0.005$. (*E*) HSM, RH30 RMS cells, and RH30 cells with knockdown for *TDP1* were grown in 2 mM VPA for 48 h. *$P < 0.05$, **$P < 0.005$. Percent cell proliferation and viability were detected using an MTT assay. (*F*) HSM, RH30 RMS cells, and RH30 cells with knockdown for *TDP1* were grown in 200 nM TSA for 48 h. *$P < 0.05$. Percent cell proliferation and viability were detected using an MTT assay.

and causes the accumulation of hTdp1–DNA covalent reaction intermediates (34). Yeast $Tdp1^{H432R}$ has been shown to cause an increase in CPT sensitivity in a Top1-dependent manner, a decrease in enzyme activity, and an accumulation of Tdp1–DNA adducts in vitro (65, 68).

In the ALF assay, we found that overexpression of $yTdp1^{H432R}$ increased CIN to a level comparable with the overexpression of wild-type yTdp1 (Fig. 4 *B* and *C*). Similar to wild-type yTdp1 overexpression, overexpression of $yTdp1^{H432R}$ also rendered cells sensitive to HU and MMS (Fig. 4*A*). In addition, in the absence of *TDP1*, the overexpression of $yTdp1^{H432R}$ increased the sensitivity to CPT (Fig. 4*A*). These experiments suggest that overexpression of $yTdp1^{H432R}$ affects the CIN and DDA-sensitivity phenotypes to a similar extent as the overexpression of wild-type yTdp1. It also suggests that Tdp1 overexpression and its CIN phenotype cause vulnerability to a broad spectrum of DNA damage-based therapeutics.

To identify candidate drug targets for cancer cells with elevated Tdp1 levels such as RMS, we performed a genome-wide SDL screen in yeast using a query strain overexpressing *TDP1* (Fig. S3*A*). We identified and validated 31 gene deletions that caused SDL upon yTdp1 overexpression (Fig. 5*A*, Fig. S3*B*, and Table S5). SDL partners were enriched for genes involved in response to DNA damage (P value $= 2.15 \times 10^{-05}$), which would be expected given the role of Tdp1 in DNA repair (69).

The class I HDAC *RPD3* was one of the genes that show an SDL interaction with the overexpression of yeast *TDP1* (Fig. 5*A*). HDACs are chromatin remodelers that remove acetylation marks from histones (70) and play a role in all processes that require structural alterations to the nucleosomes such as transcription, DNA repair, and replication (71). The human homologs of *RPD3*, *HDAC1*, and *HDAC2* are overexpressed in several tumor types, and histone deacetylase inhibitors (HDACIs) are actively being pursued as anticancer therapeutic agents (72). VPA is an FDA-approved

HDACI that is used to treat epilepsy and bipolar disorder (73) and has demonstrated potent antitumor effects against several tumor types including renal and pancreatic cancer (74, 75). The antifungal agent TSA is another well-established HDACI also with potent antitumor activity (76–78). We examined whether the SDL interaction between *RPD3* LOF and the overexpression of y*TDP1* can be recapitulated using VPA and TSA. In liquid growth assays, yeast cells overexpressing Tdp1 are more sensitive to both VPA and TSA compared with the vector-alone control (Fig. 5*B*). To see if this interaction is conserved in human cells, we next exposed the HT1080 HAC-GFP cell line overexpressing h*TDP1* to several concentrations of both deacetylase inhibitors. HT1080 cells overexpressing h*TDP1* were indeed more sensitive to both VPA and TSA (Fig. 5 *C* and *D*). Similarly, the RH30 RMS cells with elevated levels of hTdp1 were more sensitive to the HDACIs, and the knockdown of *TDP1* partially suppressed this sensitivity (Fig. 5 *E* and *F* and Fig. S3 *C* and *D*). These experiments show that SDL interactions from yeast can be recapitulated in human cells and indicate that HDACIs may be effective in specifically targeting tumors with elevated levels of Tdp1.

Discussion

Gene Overexpression Causes Genome Instability in Yeast and Uncovers a Distinct Set of dCIN Genes. Systematic phenotype screens for LOF (11) and ROF (10) alleles of CIN genes have been valuable in identifying and characterizing CIN genes in yeast and humans (9, 48, 79). Here we have complemented the CIN gene list with genes that cause CIN when overexpressed and the combined catalog of genes causing CIN, therefore, amounts to 913 genes, consisting of 692 CIN genes and 290 dCIN genes.

Similar to the CIN gene set, the dCIN gene set is enriched for processes known to be involved in genome stability, such as DNA damage repair, chromosome segregation, cell-cycle regulation, and transcription (Fig. 1*B*). We also identified genes in pathways that have recently been linked to genome stability such as metabolism (80) as well as processes not directly involved in genome stability but that have been observed previously, such as protein trafficking (10, 11). For ∼35% of the dCIN genes that function in predictable pathways such as DNA repair, replication, and mitosis and the 25% that function in or near DNA pathways known to affect genome stability such as transcription, nuclear transport, and RNA processing, their involvement in genome stability may be direct. The role in genome stability may be indirect for the remaining 40% of the genes. Regardless, the mechanisms of dCIN will require further experiments for most genes and cellular pathways identified in this study.

There is little overlap between our screens and the two previous overexpression screens, similar to the lack of overlap between the two previous screens (12, 13). The differences could be due to the methods chosen for gene overexpression and the CIN assay of choice. Zhu and coworkers used the MoBY-ORF collection (81), where genes were expressed from a high copy plasmid with the endogenous promoters, whereas Ouspenski et al. (12) used a cDNA collection expressed from a galactose inducible promoter. In addition, both these studies only used the CTF assay, and we show that 93 of the 245 dCIN genes were unique to the ALF screen.

Our phenotypic analysis of the 67 genes that are both dCIN and CIN (Fig. 2*A*) revealed that overexpression of 32 of the 67 genes recapitulated a negative genetic interaction, implying that in these cases overexpression may phenocopy LOF (Fig. 2*B* and Table S2). One explanation for this overlap is the disruption of stoichiometry in a multisubunit complex, where overexpression of one complex subunit may titrate shared factors away from the complex or sequester a subset of components, thereby disrupting a multiprotein complex (82, 83). *NUP170* is one such example where both deletion and the overexpression disrupt the nuclear pore (84). In this case, we would expect enrichment for components of protein complexes in the 32 genes that recapitulated negative GIs. However, only 8 of the 32 genes were known members of a protein complex. Therefore, in agreement with previous studies (82), we did not find a strong association between overexpression of genes that phenocopied LOF or ROF and proteins that are annotated to be components of complexes.

Further analysis of additional phenotypes, which included sensitivity to DDAs (Table S3) and formation of Rad52 foci (Table S3 and Fig. 2*F*), revealed that for 23 of the 67 CIN/dCIN genes, the phenotypic concordance was limited to the CIN phenotype. Therefore, it is possible that overexpression in these cases results in a gain-of-function phenotype (82); however, further tests will be necessary to assess this possibility.

dCIN Genes from Yeast Can Be Used to Identify dCIN Genes in Humans. Gene amplification and overexpression are common features in human cancers, and their roles in tumor progression have not been broadly investigated. We generated a list of human homologs of yeast dCIN genes to uncover amplified and/or overexpressed genes that may be relevant to tumorigenesis. Our list contains two previously characterized dCIN genes in humans (51, 52, 85) as well as eight genes whose overexpression had a clear role in cancer progression (86). Our candidate testing approach identified two additional genes, meaning that 20% (4/20) of yeast dCIN genes were phenotypically conserved in humans. However, it is likely this is an underestimate of the conservation in humans of the dCIN phenotypes observed in yeast, as screening using the HAC-GFP likely only tests for whole chromosome loss. In yeast, for example, multiple genome instability assays were used and were needed to identify the full spectrum of yeast CIN genes (10, 11).

To our knowledge, *TDP1* and *TAF12* are two dCIN genes in humans that have not previously been linked to CIN (Fig. 3*B*). *TAF12* (or transcription initiation factor IID subunit 12) is a component of the TFIID general transcription factor that is involved in RNA polymerase II-dependent transcription (87). Transcription is a process that has many links to genome instability, and aneuploidy-induced transcriptional changes are just one possible method used by cancer cells to escape cellular homeostasis mechanisms (88). Recent work identified *TAF12* as an oncogene involved in the formation of choroid plexus carcinomas, a frequently lethal brain tumor (55).

Tdp1 expression is increased in several specific types of cancers including non-small cell lung cancers (58), Dukes C colorectal cancers (57), breast cancer cell lines (89), and some RMSs (56). We show that high levels of CIN in RH30 RMS cells can be partially rescued by the knockdown of *TDP1* (Fig. 3*D*), suggesting that Tdp1 is indeed partly responsible for the CIN phenotype in these cells. This also implies that the high CIN seen in certain subtypes of RMSs may be due, at least in part, to Tdp1 overexpression (90).

SDL Screens as a Platform to Identify Therapeutic Targets in Cancers with dCIN Gene Overexpression. Given that CIN represents a vulnerability that can be exploited as a therapeutic avenue for treatment of cancer (88, 91, 92), the dCIN gene list introduces potential biomarkers for therapies that target CIN either using conventional genotoxic approaches or by exploiting synthetic lethal interactions with overexpressed genes in tumors. The overexpression of 69 dCIN genes showed sensitivity to at least one of the four DDAs tested, and ∼65% of these genes have human orthologs (Table S3). It may be possible to use these sensitivity profiles to predict drug sensitivities of tumors that are overexpressing dCIN gene orthologs and use genotoxic DDAs to augment treatment of these tumors, just as DDAs are used to treat cancers with mutations in genes that affect genome stability (93).

Another approach is to exploit SL interactions between LOF mutations and overexpressed genes, a genetic interaction termed SDL. Here we screened for SDL partners with overexpression of Tdp1, and found several SDL partners associated with overexpression of Tdp1 [despite the fact that *tdp1Δ* has few SL/SS interactions (SGD)]. These SDL partner genes were involved in DNA metabolism as expected, and many of these proteins, such as Wss1, Rad27, Slx4, and Mus81, function together with or in parallel pathways to Tdp1, suggesting that cells with high Tdp1 levels rely on other pathways to repair DNA damage.

Removal of *RPD3*, a HDAC, had a SDL interaction with *TDP1*, and this interaction could be reproduced using HDACIs VPA and TSA (Fig. 5*B*). This SDL interaction is also conserved in human cells with elevated levels of Tdp1, as both HT1080 cells overexpressing *TDP1* and RH30 cells with elevated levels of Tdp1 are sensitive to both VPA and TSA (Fig. 5 *C*–*F*). These experiments suggest that tumors with high levels of Tdp1 may be more susceptible to HDACIs.

In addition to the contribution of Tdp1 overexpression to CIN, increased levels of Tdp1 in cancer are of interest in clinical trials as a potential mechanism for the inefficacy of the Top1 poison Irinotecan (94–96). In yeast, we and others have found that direct Tdp1 overexpression surprisingly does not provide resistance to the related Top1 poison CPT. Instead, high levels of wild-type yTdp1 lead to sensitivity to a broad spectrum of adduct-forming agents and DDAs including CPT, HU, MMS, bleomycin, and HDACIs (Fig. 4*A*, Fig. 5*B*, and ref. 65). A role for yTdp1 overexpression causing DNA damage or limiting repair is further supported by the results of our SDL screen, which found that Tdp1 overexpressing yeast cells could not grow in the absence of several DNA repair factors (Fig. 5*A*). This suggests that cells with high yTdp1 are dependent on DNA repair enzymes, especially endonucleases like Rad27, Slx4, and Mus81. We also found that overexpression of the yTdp1^{H432R} mutant had similar CIN levels and sensitivity profiles compared with the overexpression of wild type, despite the reduced activity and increased adduct-forming ability of the mutant (Fig. 4 *A*–*C*). It is possible that overexpression of *TDP1* leads to the accumulation of nonspecific Tdp1–DNA adducts, and in a manner similar to Top1–DNA adducts, these may lead to DNA double-strand breaks resulting from the collision of the replication fork with the protein–DNA adducts, increasing DNA damage and CIN (61, 97).

These findings may have implications for the development of Tdp1 inhibitors. First, the dCIN phenotype induced by Tdp1 overexpression could affect the efficacy of drug response. As well, the biochemical assays used to screen for Tdp1 inhibitors rely on catalytic activity, with the most potent Tdp1 inhibitors uncovered to date being nonhydrolysable substrate mimetics (89, 98, 99). But these inhibitors may not be effective in vivo if only Tdp1 activity is targeted without influencing the affinity of Tdp1 binding to the DNA.

Although SDL has been used to identify protein targets of enzymes (82, 100, 101) and to identify specific subsets of genes within chromosome segregation mutants (29), it is underused to uncover genetic contexts that could selectively target cancer cells with elevated levels of a specific gene (26, 27, 102). SDL screens therefore represent a powerful approach for fast and easy identification of candidate chemotherapeutic drug targets within the context of dCIN gene overexpression that could enable targeted elimination of these cells. It will perhaps open avenues for repurposing existing Food and Drug Administration-approved inhibitors to target specific tumor types or the development of new cancer drugs that target druggable SDL partner genes.

Conclusions

We present here a platform using the model organism yeast to identify dCIN genes that can be leveraged to detect and characterize cognate dCIN genes in cancer. This dataset may provide insight into overexpressed genes that contribute to tumor progression by causing CIN, partly addressing the challenge of uncovering driver genes within SCNAs that would require functional testing (17, 31). The specific genotypes of individual cancer cells often will define their sensitivity profiles to chemotherapeutics (103). Determining whether gene overexpression causes CIN in well-characterized cancer cells will reveal which of these genetic vulnerabilities could be exploited in a given tumor type (104). Combining dCIN with SDL in a cross-species approach therefore offers the potential to expand the chemotherapeutic space in a more high-throughput fashion and can be used to target such cancer cell vulnerabilities.

Materials and Methods

Yeast Strains, Growth Conditions, and Plasmids. The *S. cerevisiae* strains and plasmids used are listed in Table S6. Standard methods and media were used for yeast growth and transformations. For the liquid growth assays, the expression of genes under the *GAL1* promoter was induced for 16 h by adding 2% (wt/vol) galactose to synthetic media lacking uracil. Synthetic minimal medium supplemented with appropriate amino acids was used for strains containing plasmids.

dCIN Screens and Confirmations.

CTF screen. For the CTF screen, the marker chromosome (*ade2-101*::NatMX and CFVII {*KANMX*, *SUP11*}) was introduced into the FLEX overexpression array (37) using a Singer RoToR as described in ref. 47. After diploid selection and sporulation, haploids that were Ura$^+$, Kan^R, and Nat^R were selected. Gene expression was induced on galactose for 2 d and tested for stability of the CF as in ref. 38. Increased loss of CF will result in a sectoring phenotype (see Fig. S1*A*). Candidate dCIN genes identified in the genome-wide screen were confirmed using direct transformations. Three independent transformants were tested for CTF and were assessed qualitatively by eye counting the number of sectored colonies.

ALF screen. The screen was performed as highlighted in Yuen et al. (11). Overexpression was induced for 2 d, and each strain was patched out on galactose in 1-cm^2 patches and mated to a *Mat a his1* tester lawn by replica plating on galactose containing media. His$^+$ prototrophs were selected on minimal media. Candidate dCIN genes identified in the genome-wide screen were confirmed using direct transformations with three independent transformants. Colonies on final plates were counted, and ratios of vector to overexpressed gene were calculated. Genes whose overexpression caused >twofold increase in CIN are reported in Table S1. For details on validations, please refer to *SI Materials and Methods*.

Sensitivity to Genotoxic Agents. Yeast strains carrying each dCIN candidate were grown in liquid media containing glucose followed by serial spot dilutions on galactose containing media with DDAs. Spot assays were quantified by eye to detect a difference in sensitivity to genotoxic agents compared with a vector-only control. Final concentrations of genotoxic agents on plates were as follows: HU (Sigma; 100 mM), MMS (Sigma; 0.001%), bleomycin (Enzo Life Sciences; 10 μg/mL), and benomyl (Sigma; 10 μg/mL). For liquid growth assays, yeast strains containing the overexpression plasmids (in triplicate) were grown to saturation in glucose containing media. Two microliters of the saturated culture were diluted into 200 μL of the appropriate media containing galactose and 2 mM valproic acid (Sigma: P4543). OD_{600} measurements were taken using a Tecan M200pro plate reader at 30-min intervals for 72 h at 30 °C. For quantitative analysis, area under the curves were calculated for each condition and normalized to the fitness of the wild-type strain containing a vector-alone control as described in ref. 105.

SDL Screens and Confirmations. A query strain with a plasmid containing GAL-*TDP1* was crossed to the yeast deletion array using synthetic genetic array (SGA) technology (47). Using a series of replica pinning steps, an output array was generated where each deletion mutation on the array was combined with the plasmid overexpressing *TDP1*. Overexpression of Tdp1 was induced by pinning on to media containing galactose, followed by data analysis as previously described (106). All interactions that met a cutoff of >20% changes in growth differential compared with a vector-alone control were chosen for validation (experimental-control values < –0.2). For confirmations, each deletion strain was transformed with plasmids containing a vector-alone control or *GAL-TDP1*, transformants were tested using serial spot dilutions, and only the confirmed interactions are reported in Fig. 5*A*.

Rad52-Foci Screen and Confirmations. The Rad52-GFP–tagged strain was introduced into a mini array consisting of 245 FLEX array plasmids (107) using SGA (47). Haploid strains derived from SGA were inoculated and induced with 2% final concentration of galactose for 6 h at 30 °C in liquid medium before imaging. Cells were imaged using an Evotec Opera high-throughput confocal microscope with a 60× objective (PerkinElmer), and CellProfiler version 1.0.5811 (108) was used to detect cells and nuclei in yeast. Genes that resulted in >10% spontaneous foci in the array-based screen were confirmed using retransformation. For details, refer to *SI Materials and Methods*.

Quantitative ALF Assays. Quantitative ALF assay was adapted from ref. 109. For more details, refer to *SI Materials and Methods*.

Cell Culture. Human fibrosarcoma HT1080 cells with alphoid^{tetO}-HAC-GFP were cultured in DMEM (Life Technologies) with 10% (vol/vol) FBS. To maintain the HAC, HT1080 cells were grown in 5 μg/mL of blasticidin (Sigma) as previously described (53). RH30 (alveolar RMS, PAX3-FOXO1) cells were cultured in DMEM

(Gibco BRL Life Technologies) supplemented with 10% heat-inactivated FBS (HyClone) and 1% antibiotic–antimycotic (Gibco BRL Life Technologies). Human skeletal myoblast cells were cultured using skBM-2 (Lonza) supplemented with 15% (vol/vol) FBS, 1% antibiotic–antimycotic, and 9 g/L D-glucose (final concentration, 10 g/L glucose). The RMS cell line was procured from the Leibniz Institute DSMZ-German Collection of Microorganisms. The HSM cell line was obtained from Lonza (XM13A1). All cells were grown at 37 °C with 5% (vol/vol) CO_2 in a humidified environment. Human tissue and material used for this study was approved by the Institutional Review Board of the University of British Columbia (H09-03301).

Gene Overexpression Using Lentiviral Vectors. Gateway-compatible lentiviral expression vectors were used to generate HT1080 HAC-GFP lines overexpressing candidate human genes (54). Clones for candidate human genes from the hORFeome 8.1 collection were sequenced and shuttled into the destination vector pLX302 PURO DEST (Addgene plasmid no. 25896) that allowed high expression levels (CMV promoter) and contained a C-terminal V5. Lentivirus was made in HEK293T cells using MISSION lentiviral packaging mix (Sigma) and Fugene 6 (Promega) optimized according to the manufacturer's instructions. Postinfection expression of the dCIN candidates was confirmed by Western blots. For details on target prioritization, refer to *SI Materials and Methods*.

HAC-GFP Assay, Flow Cytometry, and FISH Analysis. To assay HAC loss, HAC-GFP cells overexpressing the dCIN candidates were grown without blasticidin selection. Cells were passaged as required (2–3 d), and samples were examined every 7 d for loss of GFP signal using flow cytometry. For flow cytometry, cells were harvested using trypsin treatment, resuspended in PBS, and green fluorescence was determined. EGFP expression was detected using a FACS Calibur (BD Bioscienes) with FACS DIVA software (BD Bioscienes). Data were analyzed using FlowJo (FlowJo, LLC). A minimum of 4×10^4 events were acquired for each sample. The presence of HAC was confirmed by FISH analysis as previously described (53).

Cell Proliferation Experiments with HDACIs. HT1080-GFP cells with *TDP1* or the vector-alone control were normalized for cell counts and plated into 96-well plates. Approximately 24 h later, VPA (Sigma) was added at concentrations of 0 mM, 0.5 mM, 1 mM, 2 mM, and 3 mM, and cells were grown for 3 d. Cells were fixed with 3.7% paraformaldehyde and stained with Hoechst 33342 before nuclei were counted using a Cellomics ArrayScan. Cell lines were normalized to the vector-alone control and compared using a two-tailed Student's *t* test. The same experimental protocol was carried out with TSA (MedChem Express) at concentrations of 1 nM, 2 nM, 3 nM, and 4 nM.

MTT Assay for RMS Cell Proliferation with HDACIs. Cell proliferation and viability were measured as previously described (56). Refer to *SI Materials and Methods* for more details.

Immunobloting. Cells were collected after trypsinization and centrifugation. Pellets were resuspended in 50 mM Tris·HCl (pH 7.5), 150 mM NaCl, 10% (vol/vol) glycerol, 1% Triton X-100, and protease inhibitors (Roche), followed by lysis using sonication and centrifugation to remove debris. Lysate proteins were separated by SDS/PAGE, were transferred to PVDF, and were blotted with the following antibodies: V5 monoclonal antibody (Invitrogen; R96025), HRP-conjugated V5 antibody (Invitrogen; R96125), Cyclin E2 (Abcam: ab32103), and Tdp1 (56).

Tdp1 siRNA Knockdown Experiments. *TDP1* was knocked down transiently by transfecting 8×10^4 cells with 100 nmol/L of pooled siRNAs (Dharmacon) in a 24-well plate using Lipofectamine 2000 (Invitrogen). Knockdown was confirmed by immunoblotting. The sequences of the siRNAs are listed in ref. 56.

Chromosome Spreads. Mitotic chromosome spreads were performed as described in ref. 48. For more details, refer to *SI Materials and Methods*.

ACKNOWLEDGMENTS. We thank Dr. Nigel O'Neil, Dr. Melanie Bailey, and Dr. Peter C. Stirling for their helpful discussion and comments. This work was supported by Canadian Institute of Health Research Grant MOP 38096 and National Institute of Health Grant RO1CA158162 (to P.H.). S.D. was supported by a Canadian Institute for Advance Research Global Fellowship and a Canadian Institute for Health Research Banting Postdoctoral Fellowship. P.H. and B.A. are senior fellows in the Genetics Networks Program at the Canadian Institute for Advanced Research. C.F.B. is a scholar of the Michael Smith Foundation for Health Research (Vancouver, Canada) and a Clinical Investigator of the Child & Family Research Institute (Vancouver, Canada).

1. Bayani J, et al. (2007) Genomic mechanisms and measurement of structural and numerical instability in cancer cells. *Semin Cancer Biol* 17(1):5–18.
2. Hanahan D, Weinberg RA (2011) Hallmarks of cancer: The next generation. *Cell* 144(5):646–674.
3. Lengauer C, Kinzler KW, Vogelstein B (1997) Genetic instability in colorectal cancers. *Nature* 386(6625):623–627.
4. Stratton MR, Campbell PJ, Futreal PA (2009) The cancer genome. *Nature* 458(7239):719–724.
5. Dewhurst SM, et al. (2014) Tolerance of whole-genome doubling propagates chromosomal instability and accelerates cancer genome evolution. *Cancer Discov* 4(2):175–185.
6. Fisher R, Pusztai L, Swanton C (2013) Cancer heterogeneity: Implications for targeted therapeutics. *Br J Cancer* 108(3):479–485.
7. Horswell S, Matthews N, Swanton C (2013) Cancer heterogeneity and "the struggle for existence": Diagnostic and analytical challenges. *Cancer Lett* 340(2):220–226.
8. McBride M, Rida PCG, Aneja R (2015) Turning the headlights on novel cancer biomarkers: Inspection of mechanics underlying intratumor heterogeneity. *Mol Aspects Med* 45:3–13.
9. Stirling PC, et al. (2012) Mutability and mutational spectrum of chromosome transmission fidelity genes. *Chromosoma* 121(3):263–275.
10. Stirling PC, et al. (2011) The complete spectrum of yeast chromosome instability genes identifies candidate CIN cancer genes and functional roles for ASTRA complex components. *PLoS Genet* 7(4):e1002057.
11. Yuen KWY, et al. (2007) Systematic genome instability screens in yeast and their potential relevance to cancer. *Proc Natl Acad Sci USA* 104(10):3925–3930.
12. Ouspenski II, Elledge SJ, Brinkley BR (1999) New yeast genes important for chromosome integrity and segregation identified by dosage effects on genome stability. *Nucleic Acids Res* 27(15):3001–3008.
13. Zhu J, et al. (2015) Single-cell based quantitative assay of chromosome transmission fidelity. *G3 (Bethesda)* 5(6):1043–1056.
14. Beroukhim R, et al. (2010) The landscape of somatic copy-number alteration across human cancers. *Nature* 463(7283):899–905.
15. Sanchez-Garcia F, et al. (2014) Integration of genomic data enables selective discovery of breast cancer drivers. *Cell* 159(6):1461–1475.
16. Vogelstein B, et al. (2013) Cancer genome landscapes. *Science* 339(6127):1546–1558.
17. Zack TI, et al. (2013) Pan-cancer patterns of somatic copy number alteration. *Nat Genet* 45(10):1134–1140.
18. Fece de la Cruz F, Gapp BV, Nijman SMB (2015) Synthetic lethal vulnerabilities of cancer. *Annu Rev Pharmacol Toxicol* 55(1):513–531.
19. Janssen A, van der Burg M, Szuhai K, Kops GJPL, Medema RH (2011) Chromosome segregation errors as a cause of DNA damage and structural chromosome aberrations. *Science* 333(6051):1895–1898.
20. Manchado E, Malumbres M (2011) Targeting aneuploidy for cancer therapy. *Cell* 144(4):465–466.
21. McLornan DP, List A, Mufti GJ (2014) Applying synthetic lethality for the selective targeting of cancer. *N Engl J Med* 371(18):1725–1735.
22. van Pel DM, et al. (2013) An evolutionarily conserved synthetic lethal interaction network identifies FEN1 as a broad-spectrum target for anticancer therapeutic development. *PLoS Genet* 9(1):e1003254.
23. Tang Y-C, Williams BR, Siegel JJ, Amon A (2011) Identification of aneuploidy-selective antiproliferation compounds. *Cell* 144(4):499–512.
24. Bryant HE, et al. (2005) Specific killing of BRCA2-deficient tumours with inhibitors of poly(ADP-ribose) polymerase. *Nature* 434(7035):913–917.
25. Farmer H, et al. (2005) Targeting the DNA repair defect in BRCA mutant cells as a therapeutic strategy. *Nature* 434(7035):917–921.
26. Bian Y, et al. (2014) Synthetic genetic array screen identifies PP2A as a therapeutic target in Mad2-overexpressing tumors. *Proc Natl Acad Sci USA* 111(4):1628–1633.
27. Megchelenbrink W, Katzir R, Lu X, Ruppin E, Notebaart RA (2015) Synthetic dosage lethality in the human metabolic network is highly predictive of tumor growth and cancer patient survival. *Proc Natl Acad Sci USA* 112(39):12217–12222.
28. Kroll ES, Hyland KM, Hieter P, Li JJ (1996) Establishing genetic interactions by a synthetic dosage lethality phenotype. *Genetics* 143(1):95–102.
29. Measday V, et al. (2005) Systematic yeast synthetic lethal and synthetic dosage lethal screens identify genes required for chromosome segregation. *Proc Natl Acad Sci USA* 102(39):13956–13961.
30. Measday V, Hieter P (2002) Synthetic dosage lethality. *Methods Enzymol* 350:316–326.
31. Davoli T, et al. (2013) Cumulative haploinsufficiency and triplosensitivity drive aneuploidy patterns and shape the cancer genome. *Cell* 155(4):948–962.
32. Yang SW, et al. (1996) A eukaryotic enzyme that can disjoin dead-end covalent complexes between DNA and type I topoisomerases. *Proc Natl Acad Sci USA* 93(21):11534–11539.
33. El-Khamisy SF, et al. (2005) Defective DNA single-strand break repair in spinocerebellar ataxia with axonal neuropathy-1. *Nature* 434(7029):108–113.
34. Interthal H, et al. (2005) SCAN1 mutant Tdp1 accumulates the enzyme–DNA intermediate and causes camptothecin hypersensitivity. *EMBO J* 24(12):2224–2233.
35. Pommier Y (2004) Camptothecins and topoisomerase I: A foot in the door. Targeting the genome beyond topoisomerase I with camptothecins and novel anticancer drugs: Importance of DNA replication, repair and cell cycle checkpoints. *Curr Med Chem Anticancer Agents* 4(5):429–434.
36. Pouliot JJ, Yao KC, Robertson CA, Nash HA (1999) Yeast gene for a Tyr-DNA phosphodiesterase that repairs topoisomerase I complexes. *Science* 286(5439):552–555.

37. Douglas AC, et al. (2012) Functional analysis with a barcoder yeast gene overexpression system. *G3 (Bethesda)* 2(10):1279–1289.
38. Spencer F, Gerring SL, Connelly C, Hieter P (1990) Mitotic chromosome transmission fidelity mutants in Saccharomyces cerevisiae. *Genetics* 124(2):237–249.
39. Strathern J, Hicks J, Herskowitz I (1981) Control of cell type in yeast by the mating type locus. The alpha 1-alpha 2 hypothesis. *J Mol Biol* 147(3):357–372.
40. Mishra PK, et al. (2011) Misregulation of Scm3p/HJURP causes chromosome instability in Saccharomyces cerevisiae and human cells. *PLoS Genet* 7(9):e1002303.
41. Sarafan-Vasseur N, et al. (2002) Overexpression of B-type cyclins alters chromosomal segregation. *Oncogene* 21(13):2051–2057.
42. Mani R, St Onge RP, Hartman JL, 4th, Giaever G, Roth FP (2008) Defining genetic interaction. *Proc Natl Acad Sci USA* 105(9):3461–3466.
43. Costanzo M, Baryshnikova A, Myers CL, Andrews B, Boone C (2011) Charting the genetic interaction map of a cell. *Curr Opin Biotechnol* 22(1):66–74.
44. Jackson SP, Bartek J (2009) The DNA-damage response in human biology and disease. *Nature* 461(7267):1071–1078.
45. Alvaro D, Lisby M, Rothstein R (2007) Genome-wide analysis of Rad52 foci reveals diverse mechanisms impacting recombination. *PLoS Genet* 3(12):e228.
46. Stirling PC, et al. (2012) R-loop-mediated genome instability in mRNA cleavage and polyadenylation mutants. *Genes Dev* 26(2):163–175.
47. Tong AH, et al. (2001) Systematic genetic analysis with ordered arrays of yeast deletion mutants. *Science* 294(5550):2364–2368.
48. Barber TD, et al. (2008) Chromatid cohesion defects may underlie chromosome instability in human colorectal cancers. *Proc Natl Acad Sci USA* 105(9):3443–3448.
49. Balakrishnan R, et al. (2012) YeastMine–An integrated data warehouse for Saccharomyces cerevisiae data as a multipurpose tool-kit. *Database (Oxford)* 2012(0):bar062.
50. O'Brien KP, Remm M, Sonnhammer ELL (2005) Inparanoid: A comprehensive database of eukaryotic orthologs. *Nucleic Acids Res* 33(Database issue):D476–D480.
51. Casimiro MC, et al. (2012) ChIP sequencing of cyclin D1 reveals a transcriptional role in chromosomal instability in mice. *J Clin Invest* 122(3):833–843.
52. Spruck CH, Won KA, Reed SI (1999) Deregulated cyclin E induces chromosome instability. *Nature* 401(6750):297–300.
53. Lee H-S, et al. (2013) A new assay for measuring chromosome instability (CIN) and identification of drugs that elevate CIN in cancer cells. *BMC Cancer* 13(1):252.
54. Yang X, et al. (2011) A public genome-scale lentiviral expression library of human ORFs. *Nat Methods* 8(8):659–661.
55. Tong Y, et al. (2015) Cross-species genomics identifies TAF12, NFYC, and RAD54L as choroid plexus carcinoma oncogenes. *Cancer Cell* 27(5):712–727.
56. Fam HK, et al. (2013) TDP1 and PARP1 deficiency are cytotoxic to rhabdomyosarcoma cells. *Mol Cancer Res* 11(10):1179–1192.
57. Yu J, Shannon WD, Watson MA, McLeod HL (2005) Gene expression profiling of the irinotecan pathway in colorectal cancer. *Clin Cancer Res* 11(5):2053–2062.
58. Liu C, et al. (2007) Increased expression and activity of repair genes TDP1 and XPF in non-small cell lung cancer. *Lung Cancer* 55(3):303–311.
59. Dagher R, Helman L (1999) Rhabdomyosarcoma: An overview. *Oncologist* 4(1):34–44.
60. Liu C, Pouliot JJ, Nash HA (2002) Repair of topoisomerase I covalent complexes in the absence of the tyrosyl-DNA phosphodiesterase Tdp1. *Proc Natl Acad Sci USA* 99(23):14970–14975.
61. Liu C, Pouliot JJ, Nash HA (2004) The role of TDP1 from budding yeast in the repair of DNA damage. *DNA Repair (Amst)* 3(6):593–601.
62. Pouliot JJ, Robertson CA, Nash HA (2001) Pathways for repair of topoisomerase I covalent complexes in Saccharomyces cerevisiae. *Genes Cells* 6(8):677–687.
63. Vance JR, Wilson TE (2002) Yeast Tdp1 and Rad1-Rad10 function as redundant pathways for repairing Top1 replicative damage. *Proc Natl Acad Sci USA* 99(21):13669–13674.
64. Kapitzky L, et al. (2010) Cross-species chemogenomic profiling reveals evolutionarily conserved drug mode of action. *Mol Syst Biol* 6:451.
65. He X, et al. (2007) Mutation of a conserved active site residue converts tyrosyl-DNA phosphodiesterase I into a DNA topoisomerase I-dependent poison. *J Mol Biol* 372(4):1070–1081.
66. Interthal H, Pouliot JJ, Champoux JJ (2001) The tyrosyl-DNA phosphodiesterase Tdp1 is a member of the phospholipase D superfamily. *Proc Natl Acad Sci USA* 98(21): 12009–12014.
67. Takashima H, et al. (2002) Mutation of TDP1, encoding a topoisomerase I-dependent DNA damage repair enzyme, in spinocerebellar ataxia with axonal neuropathy. *Nat Genet* 32(2):267–272.
68. Gajewski S, et al. (2012) Analysis of the active-site mechanism of tyrosyl-DNA phosphodiesterase I: A member of the phospholipase D superfamily. *J Mol Biol* 415(4):741–758.
69. Robinson MD, Grigull J, Mohammad N, Hughes TR (2002) FunSpec: A web-based cluster interpreter for yeast. *BMC Bioinformatics* 3:35.
70. Kurdistani SK, Grunstein M (2003) Histone acetylation and deacetylation in yeast. *Nat Rev Mol Cell Biol* 4(4):276–284.
71. Shahbazian MD, Grunstein M (2007) Functions of site-specific histone acetylation and deacetylation. *Annu Rev Biochem* 76(1):75–100.
72. West AC, Johnstone RW (2014) New and emerging HDAC inhibitors for cancer treatment. *J Clin Invest* 124(1):30–39.
73. Reynolds MF, Sisk EC, Rasgon NL (2007) Valproate and neuroendocrine changes in relation to women treated for epilepsy and bipolar disorder: A review. *Curr Med Chem* 14(26):2799–2812.
74. Shi P, et al. (2014) Valproic acid sensitizes pancreatic cancer cells to natural killer cell-mediated lysis by upregulating MICA and MICB via the PI3K/Akt signaling pathway. *BMC Cancer* 14(1):370.
75. Yang FQ, et al. (2014) VPA inhibits renal cancer cell migration by targeting HDAC2 and down-regulating HIF-1α. *Mol Biol Rep* 41(3):1511–1518.
76. Vigushin DM, et al. (2001) Trichostatin A is a histone deacetylase inhibitor with potent antitumor activity against breast cancer in vivo. *Clin Cancer Res* 7(4):971–976.
77. Chang J, et al. (2012) Differential response of cancer cells to HDAC inhibitors trichostatin A and depsipeptide. *Br J Cancer* 106(1):116–125.
78. Moreira JMA, Scheipers P, Sørensen P (2003) The histone deacetylase inhibitor Trichostatin A modulates CD4+ T cell responses. *BMC Cancer* 3(1):30.
79. McManus KJ, Barrett IJ, Nouhi Y, Hieter P (2009) Specific synthetic lethal killing of RAD54B-deficient human colorectal cancer cells by FEN1 silencing. *Proc Natl Acad Sci USA* 106(9):3276–3281.
80. Shaukat Z, et al. (2015) Chromosomal instability causes sensitivity to metabolic stress. *Oncogene* 34(31):4044–4055.
81. Ho CH, et al. (2009) A molecular barcoded yeast ORF library enables mode-of-action analysis of bioactive compounds. *Nat Biotechnol* 27(4):369–377.
82. Sopko R, et al. (2006) Mapping pathways and phenotypes by systematic gene overexpression. *Mol Cell* 21(3):319–330.
83. Veitia RA (2005) Gene dosage balance: Deletions, duplications and dominance. *Trends Genet* 21(1):33–35.
84. Flemming D, et al. (2009) Two structurally distinct domains of the nucleoporin Nup170 cooperate to tether a subset of nucleoporins to nuclear pores. *J Cell Biol* 185(3):387–395.
85. Caldon CE, et al. (2013) Cyclin E2 induces genomic instability by mechanisms distinct from cyclin E1. *Cell Cycle* 12(4):606–617.
86. Santarius T, Shipley J, Brewer D, Stratton MR, Cooper CS (2010) A census of amplified and overexpressed human cancer genes. *Nat Rev Cancer* 10(1):59–64.
87. Mengus G, et al. (1995) Cloning and characterization of hTAFII18, hTAFII20 and hTAFII28: Three subunits of the human transcription factor TFIID. *EMBO J* 14(7):1520–1531.
88. Giam M, Rancati G (2015) Aneuploidy and chromosomal instability in cancer: A jackpot to chaos. *Cell Div* 10(1):3, 10.1186/s13008-015-0009-7.
89. Dean RA, et al. (2014) Identification of a putative Tdp1 inhibitor (CD00509) by in vitro and cell-based assays. *J Biomol Screen* 19(10):1372–1382.
90. Goldstein M, Meller I, Issakov J, Orr-Urtreger A (2006) Novel genes implicated in embryonal, alveolar, and pleomorphic rhabdomyosarcoma: A cytogenetic and molecular analysis of primary tumors. *Neoplasia* 8(5):332–343.
91. Bakhoum SF, Compton DA (2012) Chromosomal instability and cancer: A complex relationship with therapeutic potential. *J Clin Invest* 122(4):1138–1143.
92. Yuen KWY (2010) Chromosome instability (CIN), aneuploidy and cancer. *Encyclopedia of Life Sciences* (John Wiley & Sons, Ltd, Chichester, UK). Available at: onlinelibrary.wiley.com/resolve/doi?DOI=10.1002/9780470015902.a0022413. Accessed February 4, 2016.
93. Helleday T, Petermann E, Lundin C, Hodgson B, Sharma RA (2008) DNA repair pathways as targets for cancer therapy. *Nat Rev Cancer* 8(3):193–204.
94. Hosoi H (2015) Current status of treatments for children with rhabdomyosarcoma in the United States and Japan. *Pediatr Int* 58(2):81–87.
95. Mascarenhas L, et al. (2010) Randomized phase II window trial of two schedules of irinotecan with vincristine in patients with first relapse or progression of rhabdomyosarcoma: A report from the Children's Oncology Group. *J Clin Oncol* 28(30):4658–4663.
96. Pappo AS, et al.; Children's Oncology Group (2007) Two consecutive phase II window trials of irinotecan alone or in combination with vincristine for the treatment of metastatic rhabdomyosarcoma: The Children's Oncology Group. *J Clin Oncol* 25(4):362–369.
97. D'Arpa P, Beardmore C, Liu LF (1990) Involvement of nucleic acid synthesis in cell killing mechanisms of topoisomerase poisons. *Cancer Res* 50(21):6919–6924.
98. Huang SN, Pommier Y, Marchand C (2011) Tyrosyl-DNA Phosphodiesterase 1 (Tdp1) inhibitors. *Expert Opin Ther Pat* 21(9):1285–1292.
99. Marchand C, et al. (2014) Biochemical assays for the discovery of TDP1 inhibitors. *Mol Cancer Ther* 13(8):2116–2126.
100. Kaluarachchi Duffy S, et al. (2012) Exploring the yeast acetylome using functional genomics. *Cell* 149(4):936–948.
101. Sharifpoor S, et al. (2012) Functional wiring of the yeast kinome revealed by global analysis of genetic network motifs. *Genome Res* 22(4):791–801.
102. Reid RJD, et al. (2011) Selective ploidy ablation, a high-throughput plasmid transfer protocol, identifies new genes affecting topoisomerase I-induced DNA damage. *Genome Res* 21(3):477–486.
103. Hart T, et al. (2015) High-resolution CRISPR screens reveal fitness genes and genotype-specific cancer liabilities. *Cell* 163(6):1515–1526.
104. Boehm JS, Golub TR (2015) An ecosystem of cancer cell line factories to support a cancer dependency map. *Nat Rev Genet* 16(7):373–374.
105. Hamza A, et al. (2015) Complementation of yeast genes with human genes as an experimental platform for functional testing of human genetic variants. *Genetics* 201(3):1263–1274.
106. McLellan JL, et al. (2012) Synthetic lethality of cohesins with PARPs and replication fork mediators. *PLoS Genet* 8(3):e1002574.
107. Hu Y, et al. (2007) Approaching a complete repository of sequence-verified protein-encoding clones for Saccharomyces cerevisiae. *Genome Res* 17(4):536–543.
108. Carpenter AE, et al. (2006) CellProfiler: Image analysis software for identifying and quantifying cell phenotypes. *Genome Biol* 7(10):R100.
109. Lévesque N, Leung GP, Fok AK, Schmidt TI, Kobor MS (2010) Loss of H3 K79 trimethylation leads to suppression of Rtt107-dependent DNA damage sensitivity through the translesion synthesis pathway. *J Biol Chem* 285(45):35113–35122.
110. Chong YT, et al. (2015) Yeast proteome dynamics from single cell imaging and automated analysis. *Cell* 161(6):1413–1424.
111. Hall BM, Ma C-X, Liang P, Singh KK (2009) Fluctuation analysis CalculatOR: A web tool for the determination of mutation rate using Luria-Delbruck fluctuation analysis. *Bioinformatics* 25(12):1564–1565.
112. Deng M (2015) FirebrowseR: An "API" client for broads "firehose" pipeline. R package version 0.2.21. Available at firebrowse.org.
113. Cerami E, et al. (2012) The cBio cancer genomics portal: An open platform for exploring multidimensional cancer genomics data. *Cancer Discov* 2(5):401–404.
114. Gao J, et al. (2013) Integrative analysis of complex cancer genomics and clinical profiles using the cBioPortal. *Sci Signal* 6(269):pl1.

Supporting Information

Duffy et al. 10.1073/pnas.1611839113

SI Materials and Methods

Validations. To eliminate false-positives, all genes identified in the genome-wide ALF or CTF screens were retested using three or more independent single colonies. Only the genes that reproduced the ALF or CTF phenotypes with all three single colonies were included in the final dCIN list. For the 212 initial ALF hits, plasmids were recovered from the yeast array and were sequenced using M13F and M13R primers. For the 50 initial hits that were unique to the CTF screen, plasmids were recovered from the haploid CTF strains and were sequenced with M13 primers. Of these 262 dCIN gene initial hits, the identity of 31 plasmids did not match the gene assigned to the well address (12% error rate). In these cases, we extracted the corresponding plasmids from the bacterial array and sequenced them to confirm gene identity. ALF and CTF phenotypes were then retested for these 31 sequenced confirmed plasmids using direct transformations. Only the genes that reproduced either an ALF or CTF phenotype (14/31 genes) were included in the final list, totaling to the final 245 dCIN genes.

Rad52-Foci Screen and Confirmations. A query strain containing endogenously expressing Rad52-GFP and Hta2-mCherry (genotype: MATa Rad52-GFP::KanMX, Hta2-mCherry::NatMX, his3Δ1, leu2Δ0, ura3Δ0) was introduced into a mini array consisting of 245 FLEX array plasmids (107) using SGA (47). Haploid strains derived from SGA were inoculated into liquid medium containing 2% raffinose and grown to saturation overnight. Saturated cultures were then diluted and grown to midlog phase in low fluorescent medium with raffinose. Cells were induced with 2% final concentration of galactose for 6 h at 30 °C. A measurement of OD_{600} was used to identify an ideal concentration of cells to image, and this volume of cell culture was transferred to PerkinElmer CellCarrier plates (PerkinElmer 6007558) and subsequently imaged using an Evotec Opera high-throughput confocal microscope with a 60× objective (PerkinElmer). Single plane confocal images of live yeast cells were recorded from four positions per well. Images from the GFP and RFP were acquired simultaneously to avoid cell movement during imaging. CellProfiler version 1.0.5811 (108) was used to detect cells and nuclei in yeast confocal images using segmentation-based approaches. Intensity, texture, and morphological measurements were extracted from each identified object. Classification was used to detect DNA damage foci in cellular objects identified and measured using CellProfiler image analysis software (110). Genes that resulted in >10% spontaneous foci in the array-based screen were confirmed using retransformation. Cells were grown to saturation in glucose media and shifted to galactose for 16 h before imaging. Cells were imaged using Zeiss Axioscope and analyzed using Metamorph (Molecular Devices). Over 300 cells were counted for each overexpressed gene, and a Student's paired *t* test with a one-tailed distribution was used to determine the *P* value.

Quantitative ALF Assay. Briefly, nine independent transformants from each strain were grown to saturation in synthetic complete media with galactose for 48 h. After normalizing the saturated cultures to an OD_{600} of 2.0 and the mating type tester strain to an OD_{600} of 10.0, equal amounts of each culture were mixed together. Cells were washed with water and were plated directly on to minimal media. Following growth at 30 °C for 3–4 d, plates were scored for the ALF frequency. ALF rates and 95% confidence intervals were determined using the Ma–Sandri–Sarkar Maximum-Likelihood Estimator method using the online Flutuation Analysis Calculator, the FALCOR program (111).

Gene Overexpression Using Lentiviral Vectors. Based on increased expression in tumors (112) and known or predicted roles in tumor progression (as an oncogene or tumor suppressor) (16, 31), we generated a diverse list of 20 candidate dCIN genes for functional testing in human cells (Table S4). Six of these genes are overexpressed (86, 112), five are predicted to be either an oncogene or a tumor suppressor (16, 31), and the remaining nine are amplified in at least one tumor type (113, 114). For genes that were not included in the hORFeome collection, we chose to test either another component of the complex or a closely related ortholog.

MTT Assay for RMS Cell Proliferation with HDACIs. Briefly, 5×10^3 cells were plated in a 96-well plate and cultured in phenol red-free media. MTT solution was prepared by dissolving 5 mg of MTT in 1 mL of 1× PBS. Following treatment, the culture media was supplemented with 10% MTT and incubated for 3 h. This was followed by a 30-min incubation of 100% DMSO. Spectrophotometry was done at 565 nm using the Wallac VICTOR2 Multilable Plate Reader (Beckman-Coulter). Cell lines were normalized to the HSM control and compared using a two-tailed Student's *t* test.

Chromosome Spreads. Actively growing cells were treated with 0.1 μg/mL colcemid for 2 h before washing, trypsinization, and adding hypotonic buffer (0.075 M KCl) for 5 min at room temperature. Cells were fixed three times with 3:1 methanol:glacial acetic acid and centrifuged at 800 rpm (Rotana 460R, Hettich) for 5 min before mounting on clean slides. Slides were stained with DAPI before acquiring images with a Zeiss Axiovert 200 microscope, a Zeiss AxiocamHR camera, and the Zeiss Axiovision imaging system. Two independent observers assessed chromosome abnormalities in each of the images.

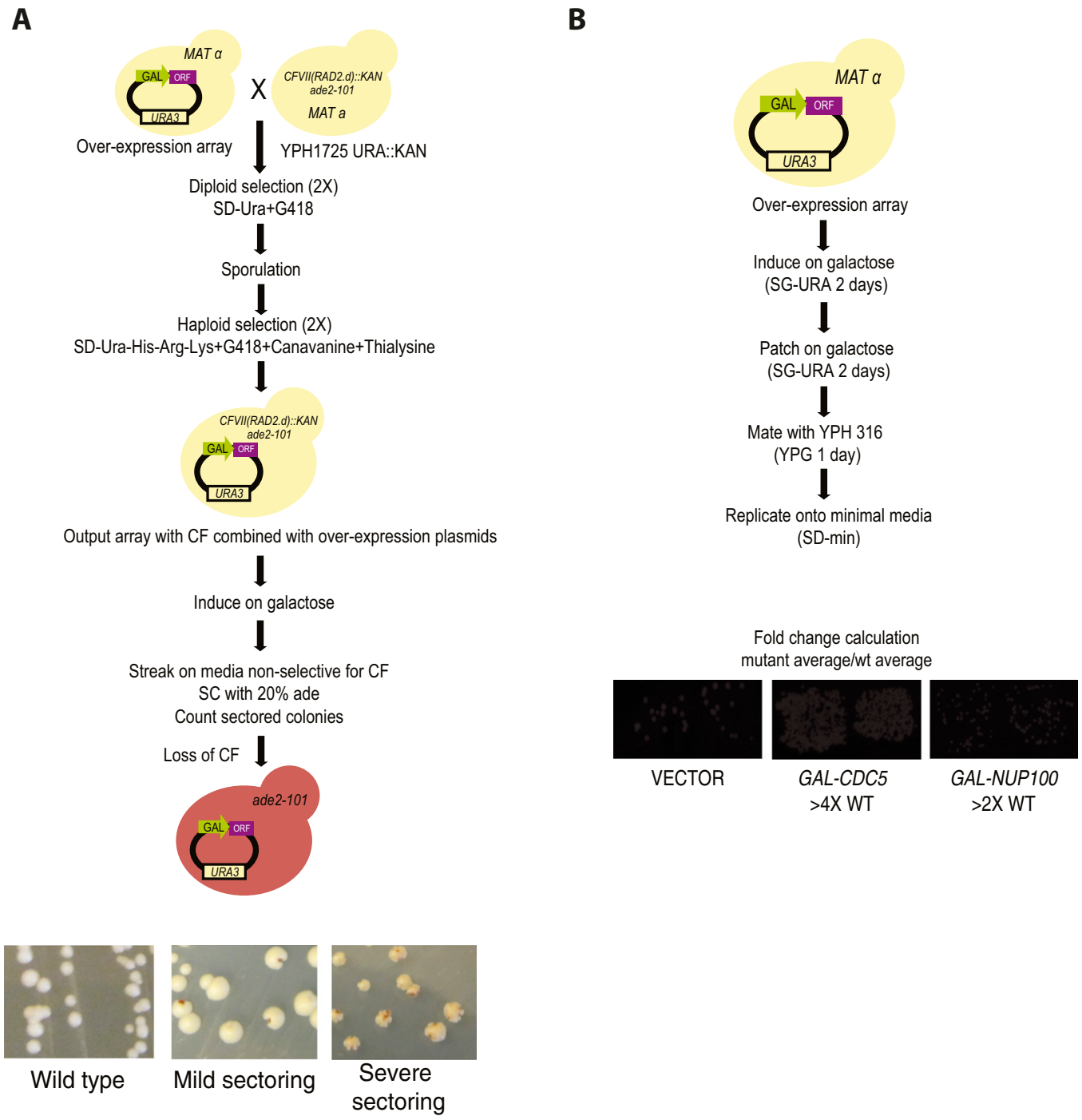

Fig. S1. Detailed schematics of the dCIN screens. (*A*) Detailed steps involved in the CTF screen. The query strain contained the *ade2-101* mutation that blocks adenine production, thus giving rise to red pigments, which is relieved by the presence of *SUP11* (*CFVII(RAD2.d)::KAN*) carried on a nonessential fragment of chromosome VII (CF). The query was mated to the full-length expression-ready (FLEX) overexpression array, and replica pinning steps on to selective media were used to select for diploids. Following sporulation, a haploid output array was generated where each overexpression plasmid was combined with the CTF query. Cells were pinned onto galactose to induce expression. After 48 h, cells were streaked on plates with low adenine media. After growing 7–10 d at room temperature, plates were placed at 4 °C for 2–3 d before scoring. Representative images of the qualitative CTF phenotypes are shown at the bottom. (*B*) The ALF screen assays the loss of the *MATα* locus in a *MATα* haploid cell. The overexpression array in a *MATα* background was pinned on galactose to induce expression. Following 48 h, the strains were induced for a second time on galactose plates in 1 cm × 1 cm patches. Cells were mated to an α-mating tester strain 2 d later. Growth of diploid, mated progeny was assessed by replica plating on minimal media and scored after 48 h. Representative images from the phenotypes assessed are shown at the bottom.

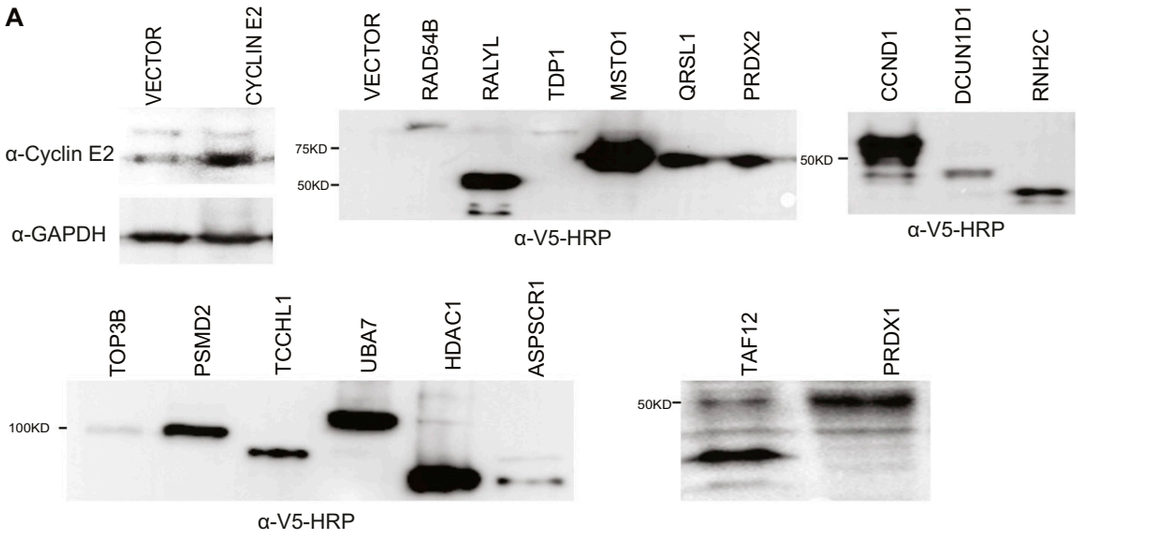

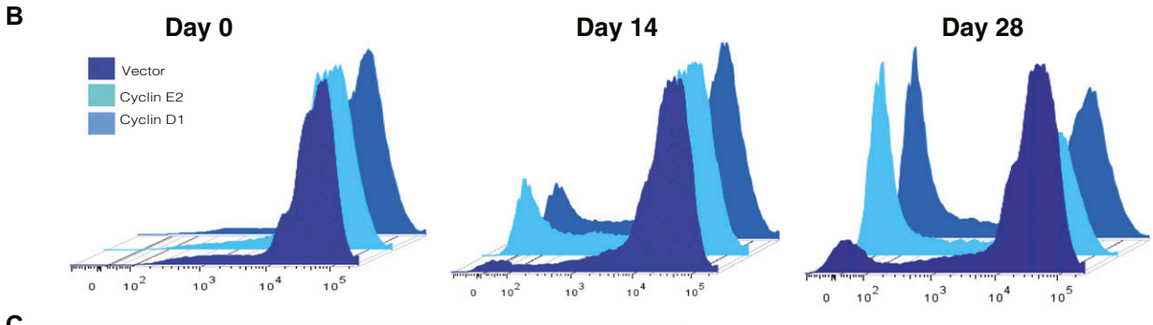

C

Sample	# of nuclei with HAC	# of nuclei without HAC	% Cells with HAC	% GFP positive cells with FACS
Vector	60	8	88.2	85
Cyclin D1	42	24	63.6	60
Cyclin E2	68	19	78.1	80

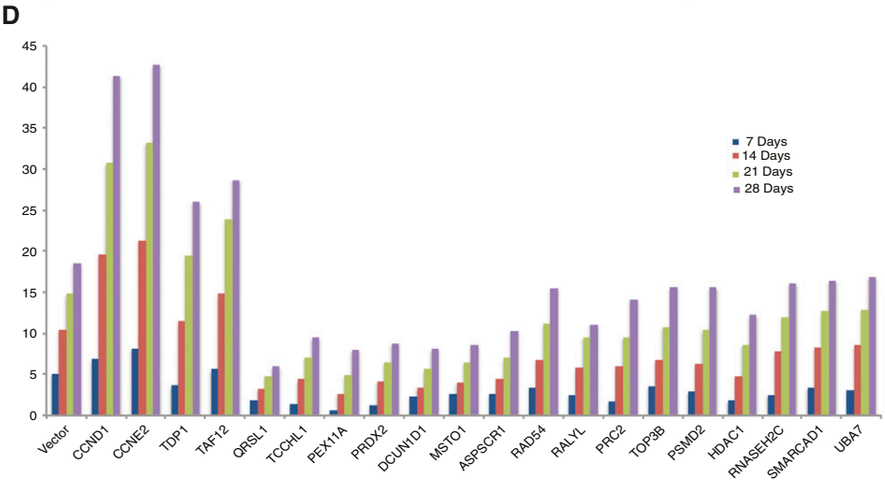

Fig. S2. Expression of the candidate dCIN genes tested in human cells. (*A*) HT1080-HAC lines overexpressing human dCIN candidate genes were assessed for protein expression using the C-terminal V5 tag. A specific antibody was used to detect Cyclin E2 levels. (*B*) Sample flow cytometry experiments of HAC-GFP lines overexpressing a vector-alone control, Cyclin D1, and Cyclin E2 at the start of the experiment, at 14 d, and at 28 d. Cells with fluorescence values below 10^3 were considered to be GFP-negative. (*C*) FISH data comparing the loss of GFP to loss of HAC from HT1080 cells. (*D*) HAC loss while overexpressing the 20 candidate human dCIN genes compared with overexpressing a vector-only control. Each bar represents measurements taken over 28 d, including 7 d (blue bars), 14 d (red bars), 21 d (green bars), and 28 d (purple bars).

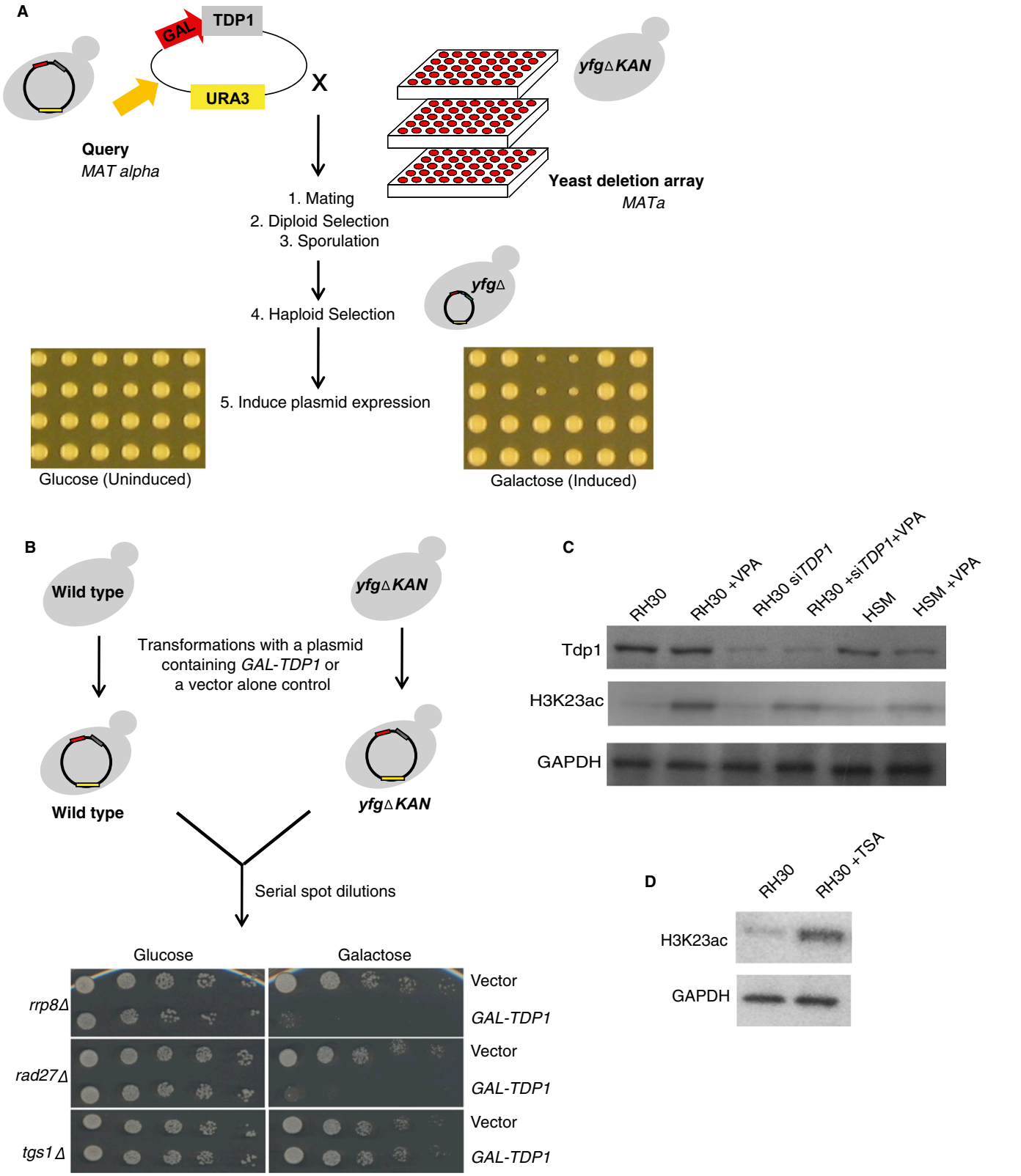

Fig. S3. SDL screens for *TDP1* and validation pipeline. (*A*) A query strain overexpressing *TDP1* was introduced into the deletion mutant array using synthetic genetic array technology. Following replica pinning steps for diploid selection and sporulation, a haploid array was generated where each deletion strain on the array was combined with the overexpression plasmid. Expression of Tdp1 was induced by pinning onto media containing galactose to detect SDL interactions. (*B*) For validations, wild-type and deletion strains were directly transformed with vector-only or *TDP1* overexpression plasmids. Growth of the transformants was assessed by serial spot dilution on either glucose- or galactose-containing medium and grown at 30 °C for 2–3 d. Overexpressing *TDP1* selectively kills mutants that lack *RAD27* and *RRP8*. (*C*) Tdp1 expression levels and acetylation levels after treatment with VPA in RMS (RH30) cells with or without *TDP1* knockdown relative to control cells (HSM). (*D*) Acetylation levels after treatment with TSA in RMS (RH30) cells.

Other Supporting Information Files

Table S1 (DOCX)
Table S2 (DOCX)
Table S3 (DOCX)
Table S4 (DOCX)
Table S5 (DOCX)
Table S6 (DOCX)